GEOPHYSICS, VOL. 71, NO. 5 (SEPTEMBER-OCTOBER 2006); P. F121–F129, 10 FIGS.
10.1190/1.2227615

Drill-bit displacement-source model: Source performance and drilling parameters

Flavio Poletto[1] and Cinzia Bellezza[1]

ABSTRACT

The emission properties of a drill-bit source and the signature of the drill-bit seismograms depend on the dynamic action of the drill bit, which in turn is a function of the geological conditions, rock properties, and drilling parameters. In fact, drilling is a variable dynamic process, in which the vibrations produced by the drill bit are transmitted into the drillstring and formation with a partition of energy determined by the impedances at the bit. In this analysis, we study drill-bit performance and calculate the forces produced by an ideal drill bit to determine the variations in the signal signature and, ultimately, the conditions of source repeatability as a function of average drilling parameters and signal frequency. The model includes near-field effects and assumes the drill bit acts as a displacement source, producing axial bit forces with relative bit/formation displacement and vertical penetration in the formation. The analysis shows that the expected bit signature, which is equivalent to the ground force in Vibroseis, depends on average tooth impact area, percussion frequency, rate of penetration, formation strength, bit wear, and downhole pressure. In particular, the results show that larger amplitudes of the axial forces are expected at a lower rate of penetration, higher formation strength, and lower formation pressure.

INTRODUCTION

The performance of the seismic while drilling (SWD) drill-bit source is analyzed in several works. In particular, Poletto (2005a, b) analyzes the energy balance of the drill-bit source. He shows that the power radiated in the far field is a fraction of the total drilling power and that the vibrations produced in the drillstring by bit/rock interaction are related to the near-field vibrations in the formation close to the bit. Poletto (2005a) uses a complex reflection coefficient to account for the boundary conditions at the bit/rock interface and to relate the near-field effects in the formation to the propagation of upgoing and downgoing waves in the drillstring. The knowledge of these drillstring waves is important because drillstring measurements typically are used as reference pilot signals for while-drilling correlation with geophone traces (Staron et al., 1988; Rector and Marion, 1991; Haldorsen et al., 1995; Miranda et al., 1996). In an early analysis, Poletto (2005a) assumes that the bit/rock contact conditions are like a simple tube acting with a given harmonic pressure over the bit area. This model assumes an ideal flat bit and does not account for bit displacement, tooth penetration (no-rate-of-penetration model; Chin, 1994), and breaking-rock effects.

In actual drilling, the bit produces displacement, with tooth penetration and rock indention caused by vertical force. The prescribed forces of a roller-cone bit are analyzed, for instance, by Biggs et al. (1969) and Eronini et al. (1982). Tooth forces of a roller-cone bit are measured by Sheppard and Lesage (1988). Breaking-rock mode and force and displacement at the bit under different pressure conditions are studied by Maurer (1965). The forces of polycrystalline diamond compact (PDC) bits are analyzed by Glowka (1986) and Langeveld (1992). In this paper, we analyze the bit as a displacement source with tooth penetration. Our analysis relates the phase of the vibrations at the bit to the drilling conditions and includes near-field vibrations and radiation of seismic waves. The phase variation of the excitation force with respect to the displacement is calculated for pilot wavelets, and the calculations allow us to estimate the repeatability and fluctuation of the drill-bit-correlated signature for a variety of configurations of drilling operational parameters and geophysical settings that may change the properties of the seismic signal. This estimation is of paramount importance for checkshot-while-drilling analysis as well as for predicting ahead of the bit (Miranda et al., 1996). Synthetic examples show the effects of rate of penetration (ROP) and of the variation of bottom-hole pressure with brittle and ductile fracturing models.

Manuscript received by the Editor September 29, 2004; revised manuscript received December 23, 2005; published online August 28, 2006.
[1]Istituto Nazionale di Oceanografia e di Geofisica Sperimentale (OGS), Borgo Grotta Gigante no. 42/c, 34010 Sgonico, Trieste, Italy. E-mail: fpoletto@ogs.trieste.it; cbellezza@ogs.trieste.it.

GENERAL THEORY

Our analysis is performed for axial waves in a homogeneous drill pipe. Without loss of generality, we neglect the drillstring response that characterizes the wave propagation in nonhomogeneous pipes with arbitrary bottom-hole-assembly (BHA) composition and top-rig boundary conditions (Paslay and Bogy, 1963; Clayer et al., 1990; Carcione and Poletto, 2000; Poletto et al., 2001). Let z be the drillstring axial coordinate. Assume a harmonic bit force F,

$$F = -\iota F_0 e^{\iota\omega t}, \tag{1}$$

acting on the formation in the (downward) positive axial direction where t is time. Let the stress σ_1 in the drillstring be expressed as a composition of downgoing and upgoing waves of frequency ω and wavenumber k, namely,

$$\sigma_1 = A\sigma_D + R\sigma_U, \tag{2}$$

where $\sigma_D = e^{\iota(\omega t - kz)}$ and $\sigma_U = e^{\iota(\omega t + kz)}$ are dimensionless downgoing and upgoing terms, respectively, and where A and R are stress coefficients. The problem is to determine A and R as a function of drilling conditions. We assume continuity at the bit/rock interface ($z \cong 0$) of the axial displacements u_1 and u_0 in the drillstring and the formation, respectively (Appendix A). If the relative displacement Δu between the formation and drillstring is zero, we have

$$\Delta u = u_0 - u_1 = 0, \tag{3}$$

and we get the result of Poletto (2005a):

$$A = \frac{F_0}{2\iota A_1}\left(-\frac{\mathcal{Z}_1}{\mathcal{Z}_b} - 1\right) \tag{4}$$

and

$$R = \frac{F_0}{2\iota A_1}\left(\frac{\mathcal{Z}_1}{\mathcal{Z}_b} - 1\right), \tag{5}$$

where A_1 is the drillstring cross section, and $\mathcal{Z}_1$ and $\mathcal{Z}_b$ are the drillstring and formation impedances, respectively. The symbol $\mathcal{Z}$ denotes integrated impedance, which is equivalent to mechanical impedance. It has the dimension of force over particle velocity (whereas radiation impedance has the dimension of stress over particle velocity). We have in the drillstring

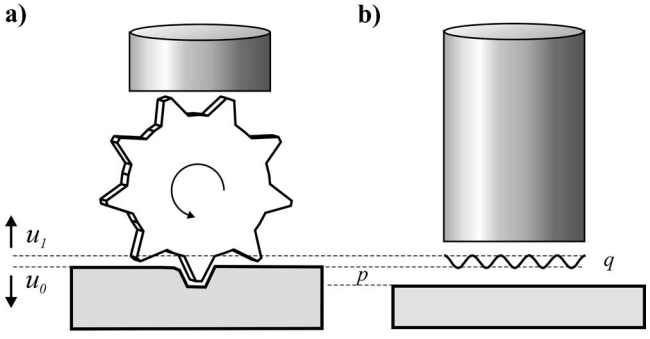

Figure 1. Concept of the bit as a displacement source. The relative displacement between the bit/string system and formation is a fraction of the tooth (chisel) height diminished by the distance penetrated during indention.

$$\mathcal{Z}_1 = A_1\rho_1 c_1, \tag{6}$$

where ρ_1 and c_1 are the density and axial rod velocity $c_1 = \sqrt{Y_1/\rho_1}$ (Kolsky, 1953) of the drillstring of Young's modulus Y_1. In the formation,

$$\mathcal{Z}_b = \frac{A_b\rho\alpha}{k_\alpha r_b}(\iota - \cot\varphi)^{-1}, \tag{7}$$

where A_b is the bit (borehole) area, r_b is bit radius, ρ is formation density, α is P-wave velocity, k_α is wavenumber, and φ is the phase of the complex impedance $\mathcal{Z}_b$. Equations 1–7 are derived by Poletto (2005a) for an ideal flat bit, without ROP, by neglecting the presence of the borehole in the low-frequency approximation, i.e., for wavelengths much larger than the borehole diameter, and treating, without loss of generality, the formation as a Poisson medium. The impedance of the formation $\mathcal{Z}_b$ is complex and accounts for the exchange of near-field (blind) and emission of far-field (radiated) powers. The formation impedance at the bit is sometimes modeled in the drilling literature by using an equivalent spring-damping system (Lutz et al., 1972; Clayer et al., 1990; Lee, 1991). The spring-damping model has the disadvantage of not explicitly representing the geophysical terms related to wave propagation. Conversely, the impedance given by equation 7 includes the formation properties and the near-field and radiation effects.

The phase φ in equation 7 is approximated at the bit/rock interface as (Poletto, 2005a)

$$\cot\varphi = -\frac{k_\alpha r_b(1 + 6\sqrt{3})}{12}. \tag{8}$$

The complex bit/rock reflection coefficient for stress is obtained from equations 4 and 5 as

$$\frac{R}{A} = -\frac{\mathcal{Z}_1 - \mathcal{Z}_b}{\mathcal{Z}_1 + \mathcal{Z}_b}. \tag{9}$$

Previous results correspond to a no-ROP model (ROP = 0). In real drilling, with ROP > 0, the relative displacement between bit and rock as well as the tooth (or cutter) penetration are important (Figure 1a). The bit is not flat, and the area A_i over which the impact force acts is, in general, different from the bit cross section A_b (Figure 2). To include the displacement effects at the bit/rock contact, instead of equation 3, we have

$$\Delta u = u_0 - u_1 \neq 0, \tag{10}$$

where Δu is now related to the bit forces and penetration during rock breaking. In this approach, the bit is assumed as a displacement source model. Off-bottom jumping effects are assumed equal to zero (sometimes denoted by the symbol $[u] = 0$). Figure 1 shows the concept of the bit acting as a displacement source. The bottom-boundary conditions of the model are analyzed with the bit acting as a harmonic source (Lee, 1991). In actual drilling conditions, even with only a single cone of only one row of teeth rotating with constant revolution speed, the prescribed tooth force is far from being a pure harmonic function because of the rock-breakage mechanism with chipping. In fact, the force-time function has different rates of variation during the indention loading phase (before rock breakage) and the unloading phase (after rock breakage) (Simon, 1963; Biggs et al., 1969; Sheppard and Lesage, 1988). Nevertheless, for simplicity we use harmonic functions for bit force and displacement. We intend that

the harmonic force represent the force variation and not the total loading force, including the gravity force, which is always positive. If we neglect the inertial forces from the moving bit mass, the vertical force F in the formation is the opposite of the axial reaction force $-F$ in the drillstring near the bit. Thus, the displacements u_1 and u_0 can be calculated with an approach similar to that used by Poletto (2005a) to obtain the results of equations 4 and 5 (Appendix A).

The relative bit/rock displacement Δu (Appendix B) is given by the bit tooth (cutter) height variation diminished by the distance penetrated by the bit tooth (Appendix C). During the indention of an ideal tooth during rotation, the relative bit/rock displacement minus the distance penetrated on average by the bit is positive. However, for the purposes of our analysis of dynamic variations, we can neglect any constant-displacement term and assume that the relative-displacement excitation is the harmonic function

$$\Delta u = q\frac{H_T}{2}e^{\iota\omega t}, \tag{11}$$

and that the harmonic force involved with the relative displacement action is

$$F = \iota F_0 e^{\iota(\omega t+\phi_F)}, \tag{12}$$

where H_T is the tooth (cutter) height (Appendix B), q ($0 \le q \le 1$) is the fraction of tooth (cutter) average exposure, complementary to penetration p (Appendix C) (Figure 1), and ϕ_F is the phase of the force in quadrature with the displacement, i.e., $\phi_F = 0$ means that the force and the displacement are out of phase by $\pi/2$. The exposure and penetration coefficients q and p are expressed as relative to tooth (cutter) height. We use the displacement equation 10 and the procedure of Poletto (2005a) to obtain (Appendix B)

$$A' = 0 \tag{13}$$

and

$$R' = -q\frac{H_T}{2}\frac{\iota\omega\mathcal{Z}_1}{A_1}\eta, \tag{14}$$

where η is given by

$$\eta = \left(1 + \frac{\mathcal{Z}_1}{\mathcal{Z}_b}\right)^{-1} \tag{15}$$

and includes the near-field and radiation effects. Figure 3 shows attributes of η^{-1}. Equations 2, 13, and 14, give the stress waves in the drillstring for a working bit. In equations 4 and 5, the bit force is produced by a downgoing drillstring wave reflected at the bit. In equations 13 and 14, the dynamic force is produced by the bit displacement as a consequence of its rotation. In the latter case, the amplitude of the downgoing drillstring wave A' is zero; if there is no relative displacement ($q = 0$), the bit force (given by the stress of amplitude R') equals zero. The upgoing stress wave in the drillstring is (Appendix B)

$$\sigma_1 = -\iota q\frac{\omega H_T}{2A_1}\frac{\mathcal{Z}_1\mathcal{Z}_b}{\mathcal{Z}_1 + \mathcal{Z}_b}e^{\iota(\omega t+k_1 z)}. \tag{16}$$

Moreover, we obtain (Appendix B)

$$F_0 = q\frac{\omega\mathcal{Z}_1 H_T}{2}\eta_0, \tag{17}$$

where

$$\eta_0 = |\eta|. \tag{18}$$

We now have

$$\phi_F = \arg\ \eta. \tag{19}$$

In this approach, we neglect the borehole in the low-frequency approximation and link the force acting over the drill-pipe cross section to the force acting over an ideal area of the formation assumed as an infinite medium. It is important to relate the magnitude of the axial bit force to the tooth (cutter) vertical displacement for realistic drilling conditions. In particular, force and displacement depend on the effective impact radius r_i and area $A_i = \pi r_i^2$ of the indentor (Figure 2). We replace bit radius and bit area in equations 7 and 8 by r_i and A_i in the calculation of the impedance $\mathcal{Z}_b$ with

$$\text{tooth radius} \le r_i \le \text{bit radius}, \tag{20}$$

giving us

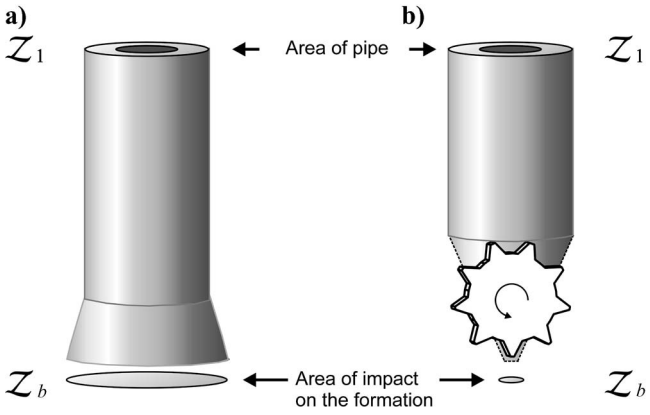

Figure 2. The impedance at the bit ($\mathcal{Z}_b$) is a function of the radius r_i (area πr_i^2) of impact on the formation. The impedance of the drillstring ($\mathcal{Z}_1$) is assumed constant.

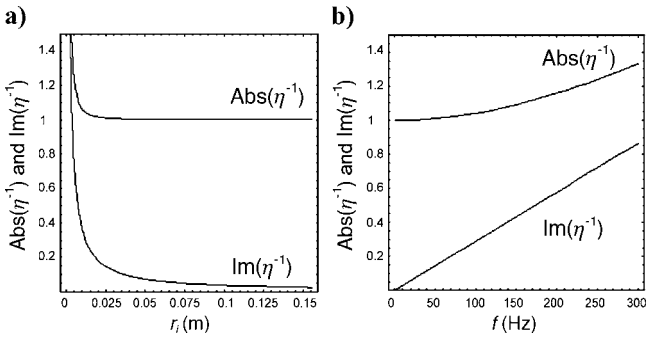

Figure 3. Absolute value and imaginary parts of the term η^{-1} representing radiation and near-field effects (a) as a function of the impact radius at a fixed frequency ($f = 50$ Hz) and (b) at a fixed impact radius ($r_i = 0.025$ m) and variable frequency.

$$\eta = \eta(r_i, \omega, \alpha, \rho; \mathcal{Z}_1). \tag{21}$$

Figure 4 shows the argument of η^{-1} as a function of impact radius and frequency.

INDENTION FORCES AND ROP

Drilling ROP is the result of the integrated action of the single indentors (cutters) producing craters with alternating action. The relation between axial penetration and vertical force needed to push one tooth or cutter indentor of unit width into the rock is (Falconer et al., 1988)

$$|F| = F_0 = \sigma \Delta z \cdot \tan\theta = \sigma_p p \frac{H_T}{2}, \tag{22}$$

where $\Delta z = pH_T/2$ is the amplitude of the harmonic depth of penetration, $\sigma_p = \sigma \tan\theta$ is a function of rock and drilling conditions, and θ is the tooth semiangle for roller-cone bits or the rake angle for PDC bits (Poletto, 2005b). If F is the tooth force per unit width, the constant σ has the dimension of a stress (rock hardness). We generalize equation 22 using equation 12 as

$$F = \iota \sigma_p p \frac{H_T}{2} e^{\iota(\omega t + \phi_F)} = \sigma_p p \frac{H_T}{2} e^{\iota[\omega t + \phi_F + (\pi/2)]}. \tag{23}$$

With the model of equation 23, we assume proportionality between force and vertical penetration of the tooth, i.e., the indention has the same phase of the force. The condition of displacement with contact, i.e., without jumping, is assumed and expressed by $[u] = 0$. The relation between q and p is given as (Appendix C)

$$q = -p\cos\phi' + \sqrt{1 - p^2 \sin^2\phi'}, \tag{24}$$

where

$$\phi' = \phi_F + \frac{\pi}{2} = \arg \iota\eta. \tag{25}$$

The phase of the harmonic revolution of the ideal tooth involved in the displacement/penetration process can be calculated as (Appendix C)

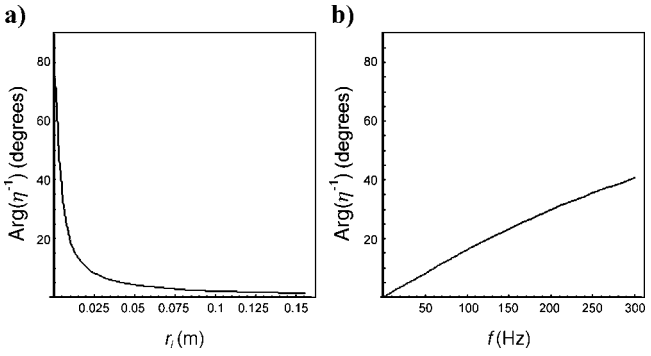

Figure 4. Phase of the term η^{-1} representing radiation and near-field effects (a) as a function of the impact radius at a fixed frequency (f = 50 Hz) and (b) at a fixed impact radius (r_i = 0.025 m) and variable frequency.

$$\phi_T = \arctan \frac{p \sin\phi'}{\sqrt{1 - p^2 \sin^2\phi'}}. \tag{26}$$

Let $H_T/2 = 1$, without loss of generality. The normalized equations relating force, displacement, and penetration become

$$\begin{cases} Fe^{-\iota\omega t} - \iota\omega \mathcal{Z}_p p e^{\iota\phi'} = 0 \\ Fe^{-\iota\omega t} - \iota\omega \mathcal{Z}_q q = 0 \\ q + pe^{\iota\phi'} = e^{\iota\phi_T} \end{cases}, \tag{27}$$

where

$$\mathcal{Z}_p = \frac{\sigma_p}{\iota\omega} \tag{28}$$

and

$$\mathcal{Z}_q = \mathcal{Z}_1 \eta \tag{29}$$

are the penetration and displacement impedances, respectively. We also define the drilling impedance as

$$\mathcal{Z}_d = \left(\frac{1}{\mathcal{Z}_q} + \frac{1}{\mathcal{Z}_p} \right)^{-1}, \tag{30}$$

which represents the ratio of the axial force F over the particle velocity $\iota\omega e^{\iota\phi_T}$ of the ideal tooth profile producing displacement. Taking the amplitudes from equation 27, we obtain the solutions

$$\begin{aligned} p &= \frac{1}{\sqrt{1 + \dfrac{\sigma_p^2}{\omega^2 \mathcal{Z}_1^2 \eta_0^2} + 2\dfrac{\cos\phi' \sigma_p}{\omega \mathcal{Z}_1 \eta_0}}} \\ &= \frac{1}{\sqrt{1 + \dfrac{|\mathcal{Z}_p|^2}{|\mathcal{Z}_q|^2} + 2\cos\phi' \dfrac{|\mathcal{Z}_p|}{|\mathcal{Z}_q|}}}, \end{aligned} \tag{31}$$

$$\begin{aligned} q &= \frac{1}{\sqrt{1 + \dfrac{\omega^2 \mathcal{Z}_1^2 \eta_0^2}{\sigma_p^2} + 2\dfrac{\cos\phi' \omega \mathcal{Z}_1 \eta_0}{\sigma_p}}} \\ &= \frac{1}{\sqrt{1 + \dfrac{|\mathcal{Z}_q|^2}{|\mathcal{Z}_p|^2} + 2\cos\phi' \dfrac{|\mathcal{Z}_q|}{|\mathcal{Z}_p|}}}, \end{aligned} \tag{32}$$

$$\begin{aligned} F_0 &= \frac{1}{\sqrt{\dfrac{1}{\sigma_p^2} + \dfrac{1}{\omega^2 \mathcal{Z}_1^2 \eta_0^2} + 2\dfrac{\cos\phi'}{\omega \mathcal{Z}_1 \eta_0 \sigma_p}}} \\ &= \frac{\omega}{\sqrt{\dfrac{1}{|\mathcal{Z}_q|^2} + \dfrac{1}{|\mathcal{Z}_p|^2} + 2\cos\phi' \dfrac{1}{|\mathcal{Z}_q \mathcal{Z}_p|}}}, \end{aligned} \tag{33}$$

and

$$\frac{q}{p} = \left| \frac{\mathcal{Z}_p}{\mathcal{Z}_q} \right|. \tag{34}$$

The nonnormalized force with a tooth of height $H_T/2$ is $F_0 H_T/2$, and the average penetration power is $W_p = F_0 p H_T^2/8$.

SYNTHETIC EXAMPLES OF SWD SIGNALS (VERTICAL FORCE)

We analyze the signals produced by vertical (axial) bit forces. Shear SH-waves produced by the gouging action of the drill bit (Poletto and Miranda, 2004) are not included in the model.

Pilot signal

SWD uses the correlation between pilot and geophone signals. A pilot wave is a reference wave propagating, typically, in the drillstring. The stress pilot wave in the drillstring is determined by force and displacement at the bit. We analyze the following drilling conditions.

Pilot waves by displacement source

The model of Poletto (2005a) neglects the borehole and assumes that the bit force acts over the bit area $A_b = \pi r_b^2$. In real drilling conditions, the bit is not flat. In the more general condition, we may assume that the area over which the vertical force acts is between the area of a single tooth and the area of the borehole (Figure 2). Thus, instead of the bit area A_b and radius r_b, we use the impact area and radius $A_i = \pi r_i^2$ and r_i, respectively (equation 20). The near-field effects are accounted for by $\eta = \eta(r_i, \omega, \alpha, \rho; \mathcal{Z}_1)$ in the near-field approximation ($kr < 1$). At low seismic frequencies (say, 30 Hz) with realistic drill collars and with A_i close to the bit area A_b, $\eta \sim 1$ and $\varphi \sim \pi/2$. For higher seismic frequencies (say, some hundred hertz) and/or A_i approximates the tooth area, the near-field effects are more important for the pilot signal. That is, the local elastic effects determine the indention depth and the elastic restitution and phase of the drillstring vibrations.

Figures 3 and 4 show the absolute value, the imaginary part, and the argument of η^{-1} (i.e., $-\phi_F$) calculated for different frequencies and contact areas. At $\phi_F = 0$, we have $p^2 + q^2 = 1$; near-field vibrations are negligible. The near-field effects become more important for smaller A_i [for analysis of drill-bit forces at the bit face, see Ma et al. (1995)] and for higher ω — say, those used for high-resolution SWD and geosteering purposes (Lesso and Kashikar, 1996). We can evaluate the importance of near-field elastic effects expressed by η by assuming that the typical ratio of the elastic rock displacement — caused by the elastic restitution after indention loading — relative to total indention depth is 0.2, as reported by Sheppard and Lesage (1988). We obtain this reference value for the example shown in Figure 4a with the impact radius $r_i = 0.015$ m, which corresponds approximately to a single-tooth radius (say, $r_i \sim r_b/10$). Using this radius, we conclude that the imaginary part of η is about 20% of its magnitude.

Pilot signal by reflection model

Assume that the relative displacement equals zero. This condition holds when $u_1 = u_0$, with $q = 0$, and is represented by equations 4 and 5. Figure 5b shows the wavelet traces of the signal propagating at different positions in the drillstring (homogeneous pipe). Near-field effects are included in this analysis. A downgoing wave propagates at negative times (before reflection) and is reflected at the bit/rock interface. An upgoing wave is recorded again at positive times. The signal is obtained with harmonic components in the bandwidth from 5–45 Hz. Figure 5a shows the corresponding model of an upgoing propagating pilot signal produced by the displacement source. The source signal is the same signal used to obtain the data of Figure 5b. This case corresponds either to perfect penetration ($\sigma_p \sim 0$ if a displacement-bit model is assumed) or to reflection of downgoing waves in the drillstring with a flat bit.

Geophone signal

A geophone signal is obtained by measuring the drill-bit wave in the formation in the far field. The radiated wavefield w can be expressed by the particle-velocity wave:

$$v_w = \frac{\partial u}{\partial t} = G(\mathbf{r})\frac{\partial F}{\partial t} = -\omega F_0 e^{\iota(\omega t + \arg \eta)} G(\mathbf{r}), \qquad (35)$$

where $G(\mathbf{r})$ is a function of the formation properties and recording position $\mathbf{r}$ (White, 1965). The compressional far-field stress is $\sigma_w = \rho\alpha v_w$. Although the phase of the force signal varies with respect to that of the relative displacement, the signature of the correlated pilot/geophone data (in frequency, given by $\sigma_w \sigma_1^*$, where * denotes conjugate) is unchanged by the variation of the bit signature because it is ultimately obtained by the correlation between signals produced by opposite reaction forces.

NOTICEABLE CASES OF PILOT SIGNALS

We analyze the case of pilot signals from vertical indention forces at the drill bit. We neglect hydraulic drilling effects and assume constant bit features.

Indention and rate of penetration

Assuming that other drilling parameters (such as bit type, crater shape, hydraulic cutting removal, and RPM) are constant, ROP is related directly to higher penetration of the single indentors. As is expected for SWD signals (Poletto and Miranda, 2004), a lower ROP corresponds to higher exposure and larger dynamic bit forces and pilot signals (Figure 6). We assume variable penetration with $0 \leq p \leq 1$. The relative displacement is obtained from equation C-3. Figure 7 shows signals calculated with different relative displacements and impact radius (area). This numerical simulation can be used to model signals of roller-cone and PDC bits. Figure 8 shows the relative displacement and the penetration at different frequencies and formation hardness. Figure 9 shows the force and the penetration power with different frequencies and formation impedance.

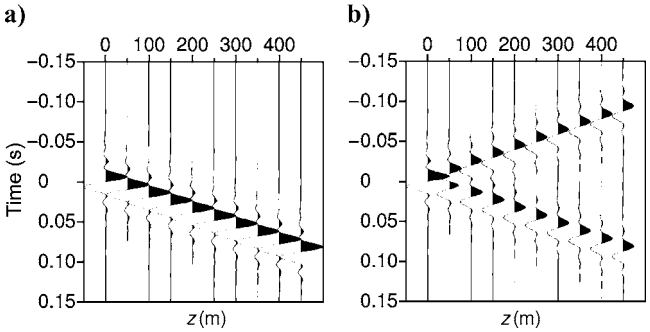

Figure 5. (a) Upgoing propagating model with displacement-bit source and (b) reflection bit model of the source pilot signal in the drillstring treated as a uniform pipe. The different traces correspond to different pipe distances.

Bit wear

Bit wear and SWD signals are discussed by Poletto (2005b). Tooth wear reduces displacement exposure by diminishing H_T. Thus, the expected pilot signal given by $F_0 H_T^{\text{wear}}/2$ is lower when tooth wear is higher (equation 17).

Pressure conditions

Pressure conditions, tooth penetration, and drilling forces are analyzed by Maurer (1965). Mud pressure is assumed higher than formation pressure. When the differential mud/formation pressures increase, the drilling fracturing mode changes, passing from brittle to ductile (Bernabe and Brace, 1990), and the force/displacement slope changes. The effect is equivalent to increasing the formation's resistance to tooth penetration, replacing σ_p in equation 22 by σ_p^{press}, which increases when the formation pressure decreases and the differential mud/formation pressure increases. The variations of the force and of the SWD signal with formation strength are shown in Figure 10 (equations 28 and 33).

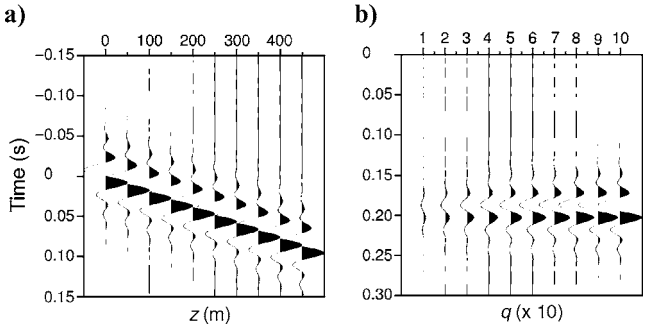

Figure 6. (a) Traces with pilot wavelets at different distances in the drillstring calculated with the upgoing propagating model of the displacement-bit source with fixed $q = 1$. (b) Traces at the same distance $z = 450$ m with variable q.

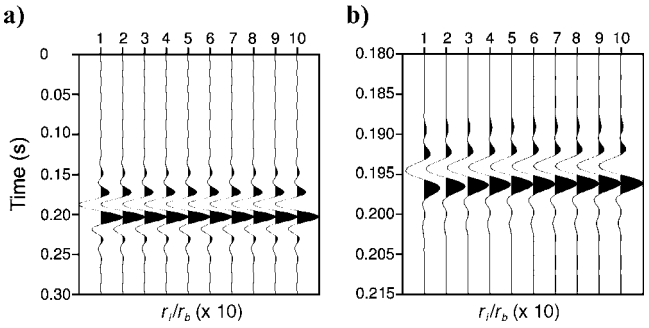

Figure 7. Traces with pilot signals calculated at the same distance in the drillstring using the upgoing propagating model of the displacement-bit source with variable impact radius r_i (plot versus r_i relative to bit radius r_b) in (a) low (10–50 Hz) and (b) higher (50–300 Hz) bandwidths. The phase of the signature varies with respect to the phase of the input displacement (assumed to be zero phase during the harmonic revolution).

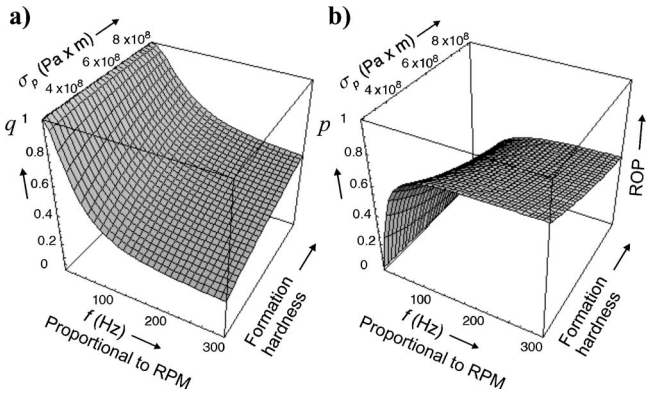

Figure 8. (a) Relative displacement q and (b) relative penetration p calculated by the force equations as a function of frequency and formation hardness. ROP is proportional to p. RPM (rotation speed) is assumed proportional to excitation frequency.

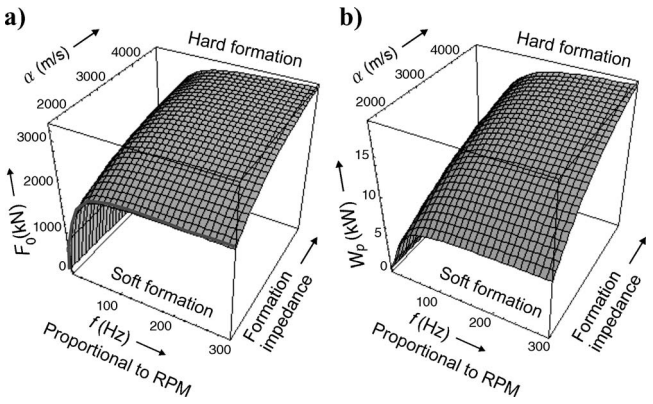

Figure 9. (a) Vertical force F_0 and (b) penetration power $F_0 p$ calculated by the normalized force equations as a function of frequency and formation compressional velocity. RPM is proportional to excitation frequency, and α is the compressional velocity of the formation.

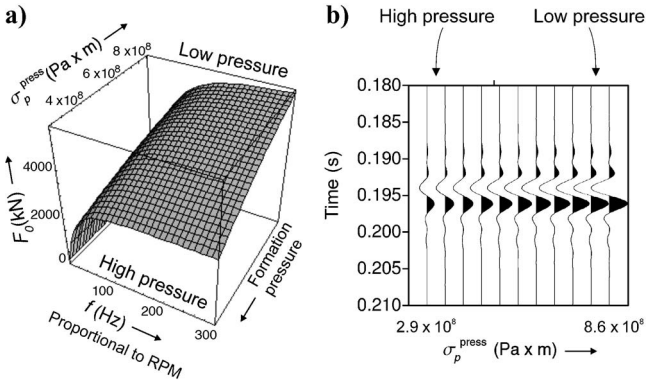

Figure 10. The variation of the differential mud/formation pressure (differential > 0) is equivalent to a variation in the formation strength to indention σ_p^{press}. In other words, the formation strength to indention increases as the differential pressure increases, i.e., when the formation pressure decreases (if we assume a constant mud pressure). (a) Variation of the bit force and (b) variation of the bit signature produced by the variation of formation pressure.

DISCUSSION

We emphasize that these models are calculated by assuming perfect cleaning drilling, without mud cuttings, flow, and hydraulic effects. In the low-frequency approximation, the borehole is neglected and the detailed distribution of the bit forces at the bit face is unknown. This leads to a simplified dynamic description of the expected performance of the bit source. The analysis is performed by treating the bit as a harmonic oscillator with displacement related to tooth exposure and penetration.

Our analysis shows that the displacement function determines at a given frequency the amplitude of the vibrations in the drillstring. Phase changes are related to the action of a single indentor. The model is discussed for roller-cone bits and is also assumed valid for PDC bits and lobed-pattern vibration modes.

CONCLUSIONS

A harmonic analysis shows the theoretical behavior of the displacement-bit model. At low seismic frequencies, the bit/rock contact is almost uninfluenced by near-field effects. The same assumption holds if the impact area is close to the cross section of the borehole. The amplitude of the pilot signature is determined by tooth exposure and, hence, tooth penetration and rock hardness. The phase between bit force and pilot-signal displacement is close to $\pi/2$. At higher frequencies, as those used for high-resolution SWD and geosteering purposes, and with small impact areas, as that of a single tooth, the near-field effects determine significant changes in drillstring signal amplitude and phase. Downhole pressure produces significant variation of signal amplitude. These changes are calculated for pilot signals measured in drillstrings.

APPENDIX A

NEAR-BIT DISPLACEMENTS

The vertical displacement in the formation near the bit, on which the force $F = -\iota F_0 e^{\iota\omega t}$ acts, can be expressed as (Poletto, 2005a)

$$u_0 = -\frac{F_0 r_b}{A_b \rho \alpha^2}(\iota - \cot\varphi)e^{\iota\omega t} = \frac{F}{\iota\omega \mathcal{Z}_b}, \tag{A-1}$$

where $\mathcal{Z}_b$ and $\cot\varphi$ are given by equations 7 and 8, respectively. We assume continuity of force at the bit/rock contact. The displacement u_1 in the drillstring, on which the reaction force

$$-F = A_1\sigma_1 \tag{A-2}$$

acts, can be expressed as (Poletto, 2005a)

$$u_1 = A\frac{\iota A_1}{\omega \mathcal{Z}_1}(\sigma_D + \sigma_U) + \frac{F_0}{\omega \mathcal{Z}_1}\sigma_U, \tag{A-3}$$

where $\mathcal{Z}_1$ is given by equation 6. Near the bit at $z \cong 0$, we have

$$u_1 = A\frac{2\iota A_1}{\omega \mathcal{Z}_1}e^{\iota\omega t} + \frac{F_0}{\omega \mathcal{Z}_1}e^{\iota\omega t} = -\frac{F}{\iota\omega \mathcal{Z}_1}\left(\frac{2\iota A_1}{F_0}A + 1\right). \tag{A-4}$$

If $\Delta u = 0$, we obtain equations 4 and 5. In fact, from equations A-1 and A-4 we have

$$\frac{F}{\iota\omega \mathcal{Z}_b} = -\frac{F}{\iota\omega \mathcal{Z}_1}\left(\frac{2\iota A_1}{F_0}A + 1\right). \tag{A-5}$$

Also, from equations 2 and A-2 we have at the bit/rock contact ($z = 0$)

$$\frac{\iota F_0}{A_1} = A + R. \tag{A-6}$$

With some manipulations, we obtain equations 4 and 5. In this case, $A = 0$ implies $F = 0$.

APPENDIX B

RELATIVE DISPLACEMENT MODEL

In the case of pure rolling of a flat cone over a flat surface, the relative displacement between drillstring and formation is constant, i.e., zero in the harmonic analysis. If the relative displacement between drillstring and formation $\Delta u = 0$, we have from equation 3 $u_1 = u_0$. From equations A-1 and A-4 we obtain the same results as Poletto (2005a), given by equations 4 and 5. In general, the drill bit acts as a forced displacement source, in which displacement is related to force and tooth penetration. The displacement-source model can be used also if the bit forces are produced by bottom-hole patterns. Let the relative displacement be

$$\Delta u = u_0 - u_1 = De^{\iota\omega t}. \tag{B-1}$$

If we assume contact between bit and formation (no drilling off bottom), the maximum (peak-to-peak) harmonic displacement is the height H_T of the tooth (cutter) indenting the rock. This is the length the tooth wedge can penetrate ideally before the bit body reaches the rock or another tooth indents the rock (Biggs et al., 1969). Conversely, equation B-1 also can be used to represent the displacement function produced by bottom-hole lobed patterns with cams of height D and no penetration effects.

The drilling process performs only by compression and does not produce traction. However, the harmonic representation of periodic force and displacement can be used for our analysis because it is equivalent to neglecting a constant shift. For tooth-induced forces, we define

$$D = q\frac{H_T}{2}, \tag{B-2}$$

where

$$0 \le q \le 1. \tag{B-3}$$

When $q = 1$, there is no tooth penetration; $q = 0$ corresponds to complete penetration. The displacement equation B-1 becomes

$$u_0 - u_1 = q\frac{H_T}{2}e^{\iota\omega t}. \tag{B-4}$$

The force can be calculated as a function of the relative displacement as

$$\frac{\partial \Delta u}{\partial t} = \frac{\partial u_0}{\partial t} - \frac{\partial u_1}{\partial t}. \tag{B-5}$$

By definition,

$$\frac{\partial u_j}{\partial t} = \frac{F}{\mathcal{Z}_j}. \tag{B-6}$$

We obtain the displacement/force relationship

$$q\frac{H_T}{2}e^{\iota\omega t} = \frac{F}{\iota\omega\mathcal{Z}_1}\left(1 + \frac{\mathcal{Z}_1}{\mathcal{Z}_b}\right), \tag{B-7}$$

where we take into account that the force F acts on the formation and the reaction force $-F$ acts on the drillstring. From equation B-7, we have

$$F = \iota q\frac{\omega\mathcal{Z}_1 H_T}{2}e^{\iota\omega t}\left(1 + \frac{\mathcal{Z}_1}{\mathcal{Z}_b}\right)^{-1}, \tag{B-8}$$

which we rewrite, according to equation 12, as

$$F = \iota F_0 e^{\iota(\omega t + \arg\,\eta)}, \tag{B-9}$$

where

$$F_0 = q\frac{\omega\mathcal{Z}_1 H_T}{2}|\eta| \tag{B-10}$$

and

$$\eta = \left(1 + \frac{\mathcal{Z}_1}{\mathcal{Z}_b}\right)^{-1}. \tag{B-11}$$

At low seismic frequencies we may assume $\mathcal{Z}_1/\mathcal{Z}_b \ll 1$. In this case, $\eta \cong 1$ and we may approximate the phase between force and relative displacement by $\pi/2$. The force of the harmonic displacement source becomes

$$F \cong \iota F_0 e^{\iota\omega t}. \tag{B-12}$$

From previous equations and from equations A-4 and A-1, we obtain the results of equations 13 and 14. These results are extended easily to the lobed-pattern case with the lobe amplitude D given by equation B-2.

APPENDIX C

TOOTH PENETRATION AND PHASE

We separate the full-tooth periodic exposure and penetration effects. Let their relative amplitudes with respect to $H_T/2$ be q and p ($0 \le q, p \le 1$), respectively. Assume there is no jumping off the bottom, i.e., the displacement without contact is $[u] = 0$. The condition of contact of the bit tooth with the formation during penetration with displacement gives

$$q + pe^{\iota\phi'} = e^{\iota\phi_T}, \tag{C-1}$$

where we assume $H_T/2 = 1$ and ϕ_T is the phase of the ideal tooth involved in the harmonic indention. Moreover, we assume that the penetration term in equation C-1 has the same phase as the force in equation 23. From equations 19 and B-9, we have

$$\phi' = \phi_F + \frac{\pi}{2} = \arg(\iota\eta). \tag{C-2}$$

From equation C-1, we have

$$q^2 + 2pq\cos\phi' + p^2 = 1, \tag{C-3}$$

and the phases of the tooth and of the penetration are related by

$$\phi_T = \arctan\frac{p\sin\phi'}{\sqrt{1 - p^2\sin^2\phi'}}. \tag{C-4}$$

From equation 22 with $\Delta z = pH_T/2$, we have the relation

$$F_0 = p\frac{\sigma_p H_T}{2}. \tag{C-5}$$

From equations B-10 and C-5 we obtain

$$\frac{q}{p} = \frac{\sigma_p}{|\eta|\omega\mathcal{Z}_1}, \tag{C-6}$$

which relates ROP to bit/rock properties in the low-frequency approximation.

REFERENCES

Bernabe, Y., and W. F. Brace, 1990, Deformation and fracture of Berea Sandstone: The brittle/ductile transition in rocks: American Geophysical Union Geophysical Monograph 56, 91–101.

Biggs, M. D., J. B. Cheatham, Jr., and U. Rice, 1969, Theoretical forces for prescribed motion of a roller bit: Society for Petroleum Engineers paper 2391.

Carcione, J. M., and F. Poletto, 2000, Simulation of stress waves in attenuating drill strings, including piezoelectric sources and sensors: Journal of the Acoustic Society of America, **108**, 53–64.

Chin, W. C., 1994, Wave propagation in petroleum engineering: Gulf Publishing Company.

Clayer, F., J. K. Vandiver, and H. Y. Lee, 1990, The effect of surface and downhole boundary conditions on the vibration of drillstrings: Society for Petroleum Engineers paper 20447.

Eronini, I. E., W. H. Somerton, and D. M. Auslander, 1982, A dynamic model for rotary rock drilling: American Society of Mechanical Engineers Journal of Energy Resources Technology, **104**, 108–120.

Falconer, I. G., T. M. Burgess, and M. C. Sheppard, 1988, Separating bit and lithology effects from drilling mechanics data: Independent Association of Drilling Contractors/Society of Petroleum Engineers paper 17191.

Glowka, D. A., 1986, The use of single-cutter data in the analysis of PDC bit design: Society for Petroleum Engineers paper 15619.

Haldorsen, J. B. U., D. E. Miller, and J. J. Walsh, 1995, Walk-away VSP using drill noise as a source: Geophysics, **60**, 978–997.

Kolsky, H., 1953, Stress waves in solids: Oxford University Press.

Langeveld, C. J., 1992, PDC bit dynamics: Independent Association of Drilling Contractors/Society of Petroleum Engineers paper 23867.

Lee, H. Y., 1991, Drillstring axial vibration and wave propagation in boreholes: Ph.D. dissertation, Massachusetts Institute of Technology.

Lesso, W. G., and S. V. Kashikar, 1996, The principles and procedures of geosteering: Independent Association of Drilling Contractors/Society of Petroleum Engineers paper 35051.

Lutz, J., M. Raynaud, S. Gastalder, C. Quichaud, and J. Raynald, J. A. Muckerloy, 1972, Instantaneous logging based on a dynamic theory of drilling: Society of Petroleum Engineers paper 3604.

Ma, D., D. Zhou, and R. Deng, 1995, The computer simulation of the interaction between roller bit and rock: Society of Petroleum Engineers paper 29922.

Maurer, W. C., 1965, Shear failure of rock under compression: Society of Petroleum Engineers paper 1054.

Miranda, F., L. Aleotti, F. Abramo, F. Poletto, A. Craglietto, S. Persoglia, and F. Rocca, 1996, Impact of seismic while drilling technique on exploration wells: First Break, 14, 55–68.

Paslay, P. R., and D. B. Bogy, 1963, Drill string vibrations due to intermittent contact of bit teeth: Journal of Engineering for Industry, Transactions of the American Society of Mechanical Engineers, 187–194.

Poletto, F., 2005a, Energy balance of the drill-bit seismic source — Part A: Rotary energy and radiation properties: Geophysics, **70**, T13–T28.

——, 2005b, Energy balance of the drill-bit seismic source — Part B: Drill bit versus conventional seismic sources: Geophysics, **70**, T29–T44.

Poletto, F., M. Malusa, and F. Miranda, 2001, Numerical modeling and interpretation of drill-string waves: Geophysics, **66**, 1569–1581.

Poletto, F., and F. Miranda, 2004, Seismic while drilling — Fundamentals of

drill bit seismic for exploration: Handbook of geophysical exploration, seismic exploration series, vol. 35, Elsevier Science Publ. Co.
Rector, J. W., III., and B. P. Marion, 1991, The use of drill-bit energy as a downhole seismic source: Geophysics, **56**, 628–634.
Sheppard, M. C., and M. Lesage, 1988, The forces at the teeth of a drilling rollercone bit: Theory and experiment: Society of Petroleum Engineers paper 18042.
Simon, R., 1963, Energy balance in rock drilling: Society of Petroleum Engineers paper 499.
Staron, P., G. Arens, and P. Gros, 1988, Method of instantaneous acoustic logging within a wellbore: U. S. patent 4 718 048.
White, J. E., 1965, Seismic waves: Radiation, transmission, and attenuation: McGraw-Hill Book Company.